doi:10.1006/jmbi.2000.4236 available online at http://www.idealibrary.com on IDEAL J. Mol. Biol. (2000) 304, 585–598

JMB

Crystal Structures of a Rab Protein in its Inactive and Active Conformations

Christopher Stroupe and Axel T. Brunger*

The Howard Hughes Medical Institute and Departments of Molecular and Cellular Physiology, Neurology and Neurological Sciences, and Stanford Synchrotron Radiation Laboratory, Stanford University, Stanford CA 94305-548, USA

**Corresponding author*

We have determined crystal structures of Sec4, a member of the Rab family in the G protein superfamily, in two states: bound to GDP, and to a non-hydrolyzable GTP analog, guanosine-5′-(β,γ)-imidotriphosphate (GppNHp). This represents the first structure of a Rab protein bound to GDP. Sec4 in both states grossly resembles other G proteins bound to GDP and GppNHp. In Sec4-GppNHp, structural features common to active Rab proteins are observed. In Sec4-GDP, the switch I region is highly disordered and displaced relative to the switch I region of Ras-GDP. In two of the four molecules of Sec4-GDP in the asymmetric unit of the Sec4-GDP crystals, the switch II region adopts a conformation similar to that seen in the structure of the small G protein Ran bound to GDP. This allows residues threonine 76, glutamate 80, and arginine 81 of Sec4 to make contacts with other conserved residues and water molecules important for nucleotide binding. In the other two molecules in the asymmetric unit, these interactions do not take place. This structural variability in both the switch I and switch II regions of GDP-bound Sec4 provides a possible explanation for the high off-rate of GDP bound to Sec4, and suggests a mechanism for regulation of the GTPase cycle of Rab proteins by GDI proteins.

Keywords: G protein; Rab; Sec4; GDP; guanosine-5′-(β,γ)-imidotriphosphate

Introduction

Many guanosine nucleotide-binding proteins couple GTP hydrolysis to structural changes that affect their affinity for regulators and effectors. These GTPases, or G proteins, use a number of conserved sequence motifs to carry out a cycle of GTP binding, GTP hydrolysis, and GDP release, with subsequent binding of GTP. The GTP-bound state of a G protein is its ''active'' state, able to exert a stimulatory or inhibitory effect on such cellular processes as membrane trafficking, the cell cycle, transmembrane signal transduction, nuclear transport, and protein synthesis by binding and modulating the activity and/or localization of effectors. After GTP has been hydrolyzed to GDP and inorganic phosphate, GDP remains bound and the protein is ''inactive'', unable to bind its targets (reviewed by Bourne *et al.*, 1990, 1991; Sprang, 1997).

Progression through the GTPase cycle is itself regulated by accessory proteins. GTPase-activating proteins (GAPs) and regulators of G protein signalling (RGS proteins) greatly increase the normally low intrinsic hydrolytic activity of G proteins (Geyer & Wittinghofer, 1997; Scheffzek *et al.*, 1998). Nucleotide release is regulated both negatively and positively: GDP dissociation inhibitors (GDIs) slow the release of GDP, while guanine nucleotide exchange factors (GEFs) increase the rate of GDP and/or GTP release (Geyer & Wittinghofer, 1997). This dual ability to regulate and to be regulated allows G proteins to act as switches that respond to signals from other proteins and regulate the function of other macromolecules accordingly.

Sec4 is a small (23.5 kDa), monomeric G protein required for the targeting and fusion of post-Golgi secretory vesicles to the plasma membrane in *Saccharomyces cerevisiae* (Salminen & Novick, 1987). It is a member of the Rab family, a branch of the G protein superfamily whose members are important for a wide variety of membrane trafficking events (Martinez & Goud, 1998; Novick & Brennwald, 1993; Pfeffer, 1994). In addition to its cycle of nucleotide binding and hydrolysis, Sec4 undergoes a cycle of localization. Sec4-GTP associates with the membranes of secretory vesicles and the plas-

E-mail address of the corresponding author: axel.brunger@stanford.edu

0022-2836/00/040585–14 $35.00/0

ma membrane *via* a geranylgeranyl moeity covalently attached to a C-terminal cysteine residue (Newman & Magee, 1993). Following membrane fusion and GTP hydrolysis, Sec4-GDP is extracted from the plasma membrane by a GDI protein that also slows the release of GDP (Novick *et al*., 1993; Walworth *et al*., 1989). Though the means by which these cycles of nucleotide binding and physical localization are coupled to vesicle targeting and fusion are unclear, proteins (Sec2 and the exocyst complex) have been identified whose interactions with Sec4 are important for delivery and targeting of vesicles to the plasma membrane (Guo *et al*., 1999; Walch-Solimena *et al*., 1996, 1997).

Both the GTP and GDP-bound states of Sec4 are recognized by regulatory factors that modulate nucleotide binding and hydrolysis, and assist Sec4 in its cycle of physical localization within the cell (Du *et al*., 1998; Garrett *et al*., 1994; Walch-Solimena *et al*., 1997). Thus, knowledge of the structure of Sec4 in its GTP and GDP-bound states is central to an understanding of the mechanism by which Sec4 is regulated and, in turn, acts as a switch regulating vesicular trafficking. To this end, we have solved the crystal structures of Sec4 bound to a non-hydrolyzable GTP analog, guanosine-5′-(β,γ)-imidotriphosphate (GppNHp), and to GDP, at resolutions of 2.0 and 1.8 Å, respectively.

Results

Structures of Sec4-GppNHp and Sec4-GDP

The variant of Sec4 we used for crystallographic studies of both the GDP and GppNHp-bound forms included residues 19-187, lacking its first 18 and last 28 residues. Known as the N and C-terminal hypervariable regions, respectively, the sequences of these regions of Sec4 are poorly conserved with respect to other G proteins, even in the Rab family (Brennwald & Novick, 1993). We will refer below to this truncated form of the protein as Sec4.

We solved and refined the structure of Sec4-GppNHp using diffraction data extending to a minimum Bragg spacing of 2.0 Å, with an R_{free} of 29.2 % and an $R_{working}$ of 26.4 %. The structure was refined using a maximum-likelihood target function, incorporating experimental phases derived from a multiple-wavelength anomalous diffraction (MAD) experiment (see Materials and Methods). The asymmetric unit contains two molecules that are related by primarily translational non-crystallographic symmetry: a translation of roughly half the *c*-axis of the unit cell. The structures of these two molecules are virtually identical (0.2 Å root-mean-square difference (rmsd) for 168 C^{α} positions; see Materials and Methods), and all of the observations we describe below apply to both molecules. The final refined model contains two Sec4 molecules, two GppNHp molecules, two magnesium ions, and 138 water molecules (Table 1 and Figure 1(a)).

We solved and refined the structure of Sec4-GDP using diffraction data to a minimum Bragg spacing of 1.8 Å with an R_{free} of 29.6 % and an $R_{working}$ of 27.9 %. Refinement was also carried out using a maximum-likelihood target function, using experimental phases derived from a MAD experiment (see Materials and Methods). The non-crystallographic symmetry of the Sec4-GDP unit cell (identical to the asymmetric unit due to the triclinic space group) also consists primarily of translations, which in this case are not coincident with any one crystallographic axis. There are four molecules in the unit cell, and though the four structures are similar overall, significant differences do exist, which will be discussed below. The final refined model contains four Sec4 molecules, four GDP molecules, eight cobalt(II) ions (see below), and 328 water molecules (Table 2 and Figure 1(b)).

The overall structures of Sec4 bound to GppNHp and GDP closely resemble those of other small monomeric G proteins such as Ras, Rab3A, and Ypt51 (Dumas *et al*., 1999; Esters *et al*., 2000; Milburn *et al*., 1990; Pai *et al*., 1990; Tong *et al*., 1991). The fold consists of a six-stranded β-sheet, with five parallel strands and one antiparallel strand, flanked by five α-helices (Figure 2(a) and (b)). The nucleotide is bound primarily by conserved regions that form several of the loops between the secondary structure elements (Bourne *et al*., 1991; Sprang, 1997).

Structural features of the Rab family G proteins Rab3A and Ypt51 that differ from Ras are also seen in the structure of Sec4-GppNHp. In particular, the conformation and position of helix α2 (which forms part of the switch II region) is nearly identical in Sec4-GppNHp, Rab3A-GppNHp, and Ypt51-GppNHp. Relative to helix α2 in Ras-GppNHp, helix α2 in all three Rab proteins is rotated around its helical axis, and its N terminus is tilted away from the remainder of the protein. Additionally, the contacts seen in Sec4 between residues in helix α2 and residues in the loop between helix α1 and sheet β2 (the switch I region) are similar to those seen in Rab3A-GppNHp and Ypt51-GppNHp (Dumas *et al*., 1999; Esters *et al*., 2000; Pai *et al*., 1990). These include packing of the alpha carbon atom of glycine 54 against the side-chains of phenylalanine 82 and isoleucine 85, as well as contacts between the side-chain of tyrosine 89 and the side-chains of tryptophan 74 and isoleucine 55. Additionally, the side-chain from serine 29 donates a hydrogen bond to the gamma phosphate atom of the nucleotide. This contact is seen in the structures of Rab3A and Ypt51 bound to GppNHp (Dumas *et al*., 1999; Esters *et al*., 2000), though not in the structure of Ras-GppNHp, since the equivalent residue in Ras is a glycine residue (Pai *et al*., 1990).

The differences between the structure of Sec4-GppNHp and the structures of Rab3A-GppNHp and Ypt51-GppNHp are primarily found in the loops between strands β2 and β3 and between helix α3 and strand β5 (Dumas *et al*., 1999; Esters

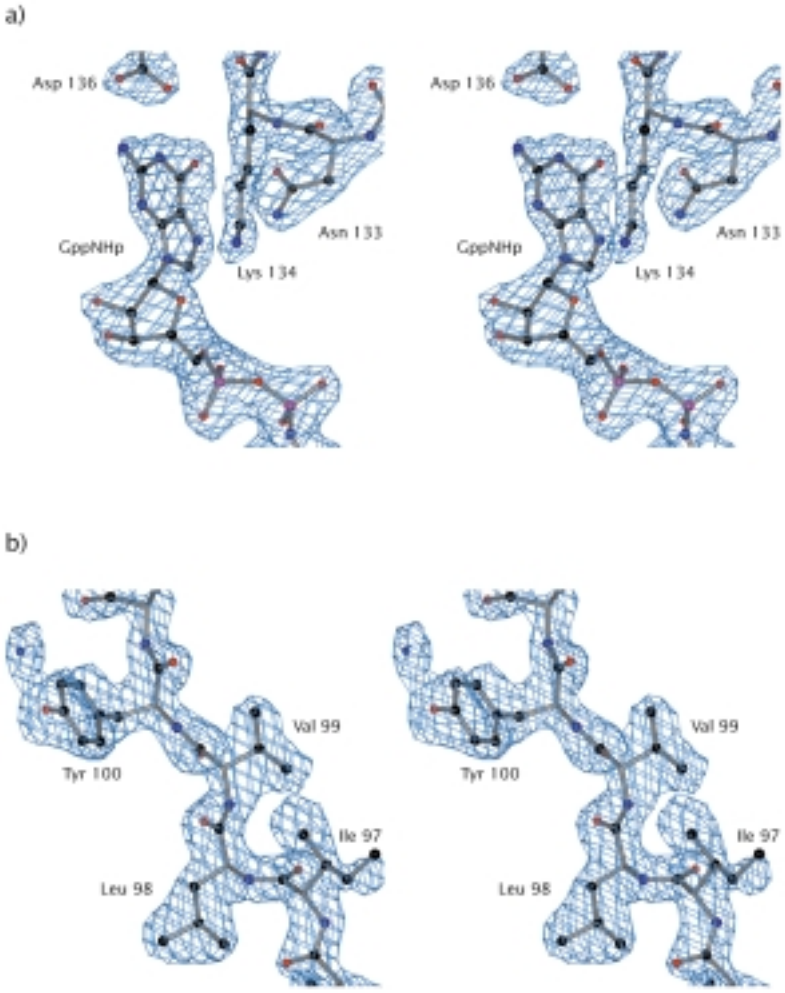

Figure 1. Representative electron density of Sec4-GppNHp and Sec4-GDP. (a) Stereoview of electron density of Sec4 bound to guanosine-5′-(β,γ)-imidotriphosphate (GppNHp), contoured at 1.5 σ, obtained from a $2F_o - F_c$ composite annealed omit map using a combination of experimental and calculated phases. The electron density is shown superimposed on the final refined model of the nucleotide and residues involved in binding the guanine base, shown as a ball-and-stick representation. (b) Stereoview of experimental, solvent-flipped and NCS-averaged electron density map, contoured at 1.5 σ, near residue valine 99 (molecule A) of Sec4-GDP. The final refined model of Sec4-GDP is shown in a ball-and-stick representation, with a water molecule represented by a blue sphere. (Figures 1 and 4(b) prepared using the programs Bobscript (Esnouf, 1997), GL_Render (courtesy of Dr L. Esser), and POV-RaY (POV-Ray Team, 1998).)

et al., 2000). These loops are partially disordered in the structures of Rab3A-GppNHp and Sec4-GppNHP, as well as Sec4-GDP (Dumas *et al*., 1999). In Ypt51-GppNHp, loop β2-β3 is stabilized by interactions with a second nucleotide bound between Ypt51 molecules in the crystal, and loop α3-β5 is stabilized by interactions between a lysine side-chain in the loop and three main-chain carbonyl oxygen atoms from helix α3 (Esters *et al*., 2000). The loop between strand β5 and helix α4 is well ordered in the structures of Rab3A-GppNHp and Sec4-GppNHp, though it contains a one-residue insertion in Rab3A (Dumas *et al*., 1999). In Ypt51, this loop contains a four-residue insertion relative to Sec4; in the crystal structure of Ypt51-GppNHp it is flexible (Esters *et al*., 2000).

Metal binding

A metal ion is bound to both Sec4-GppNHp and Sec4-GDP; this is also seen in other G proteins (Sprang, 1997). We modeled the metal ion as Mg^{2+} in the Sec4-GppNHp structure, as Mg^{2+} is required for nucleotide binding by Sec4 (Kabcenell *et al*., 1990) and was included in the crystallization buffer. In the Sec4-GDP complex we modeled a Co^{2+} instead; 35 mM $CoCl_2$ was included in the crystallization buffer for Sec4-GDP, as the presence of cobalt was required for growth of large, single crystals. Also, significant electron density in an anomalous difference map can be seen in the Mg^{2+}-binding site. We interpreted this anomalous density as being due to a Co^{2+}, since cobalt has a much higher anomalous signal than magnesium at the X-ray wavelength at which data was collected. We do not expect that this substitution has any substantial effect on the structure, as the octahedral coordination geometry of Co^{2+} in our structure is not significantly different from that of Mg^{2+} in other protein structures (Metalloprotein Structure and Design Group, 1998). Additionally, it was possible to grow crystals of Sec4-GDP in the absence of $CoCl_2$, though the crystals tended to grow in clusters rather than as single crystals.

In Sec4-GppNHp, the coordinating ligands of the Mg^{2+} consist of one oxygen atom each from the β and γ-phosphate atoms of the nucleotide, two water molecules, and the side-chain hydroxyl groups of serine 34 and threonine 52. In Sec4-GDP, two water molecules take the place of the oxygen atom from the γ-phosphate and the side-chain hydroxyl group of threonine 52. These contacts are

Table 1. Summary of crystallographic data for Sec4-GppNHp

	Inflection (λ2)	Peak (λ1)	High (λ4)	Native
A. *Data collection statistics:*				
Wavelength (Å)	0.9802	0.9800	0.9537	1.2843
Resolution (Å)[a]	23.8-2.7(2.8-2.7)	23.8-2.7(2.8-2.7)	23.8-2.7(2.8-2.7)	38.0-2.0 (2.07-2.0)
#observations	54,997	60,629	53,495	87,371
Unique	18,613	18,621	18,702	23,496
% complete	98.6(93.9)	99.4(98.7)	98.1(91.5)	99.7(99.4)
R_{sym}[b]	0.074(0.336)	0.071(0.310)	0.097(0.692)	0.091(0.624)
I/σ	16.1(3.7)	16.3(4.0)	12.4(1.8)	13.2(2.2)
a,*b*,*c*,α,β,γ		83.724,83.724,87.223,90,90,120		84.504,84.504,86.469,90,90,120
source/detector		ALS 5.0.2/Quantum-4		NSLS X4A/R-AXIS IV
B. *Anomalous phasing statistics:*				
MAD phasing power[c]				
	λ_2-λ_1^+	λ_2-λ_1^-	λ_2-λ_2^-	
23.8-2.7 Å (2.8-2.7 Å)	0.55 (0.26)	0.89 (0.34)	0.50 (0.27)	
SAD phasing power				
	λ_1-λ_1^-	λ_2-λ_2^-	λ_4-λ_4^-	
23.8-2.7 Å (2.8-2.7 Å)	0.83 (0.17)	0.12 (0.00)	0.18 (0.01)	
Figures of merit[d]	23.8-2.7 Å (2.8-2.7 Å)			
λ_2-λ_1 MAD	0.33 (0.13)			
λ_1 SAD	0.20 (0.04)			
λ_2 SAD	0.12 (0.00)			
λ_4 SAD	0.05 (0.00)			
Combined figure of merit	0.38 (0.13)			
C. *Model statistics*				
Resolution	38.0-2.0 Å (2.07-2.0 Å)		#protein residues	336
R_{free}[e]	0.2916(0.3796)		#Mg^{2+}	2
$R_{working}$	0.2636(0.3754)		#GppNHp molecules	2
rms deviation, bonds Å	0.0068		#water molecules	138
rms deviation, angles (deg)	1.1531			
rms deviation, dihedrals (deg.)	22.6436			
rms deviation, impropers (deg.)	0.7507°			
Most-favored phi-psi (%)	86.9			
Luzatti coordinate error cross-validated (Å)	0.34			
Luzatti coordinate error (Å)	0.37			
σ_A coordinate error (Å)	0.35			
σ_A coordinate error (Å) cross-validated	0.36			
Average *B*-factor (Å^2)	34.1192			
Range of *B*-factors (Å^2)	11.6197 - 66.2497			

[a] Values in parentheses are for the high-resolution bin.

[b] $R_{sym} = \Sigma_h \Sigma_i |I_i(h) - \langle I\ (h)\rangle| / \Sigma_h \Sigma_i\ I_i(h)$ where $I_i(h)$ is the *i*th measurement and $\langle I\ (h)\rangle$ is the mean of all measurements of $I(h)$ for Miller indices *h*.

[c] MAD phasing power is defined as $[\langle |F_D - F_N|^2\rangle / \int_\phi P(\phi)(||F_N\ |e^{i\phi} + \Delta F_h| - |F_D\ |)^2 d\phi]^{1/2}$ where $P(\phi)$ is the experimental phase probability distribution. F_N corresponds to the structure factors at the reference wavelength, F_D corresponds to the structure factors at wavelength λ_i (indicated by a superscript +) or its Friedel mate (indicated by a superscript −), and ΔF_h is the difference in heavy atom structure factors between the two wavelengths. SAD phasing power is the same except the reference wavelength is λ_i.

[d] Figure of merit $= \int_\phi P(\phi) e^{i\phi} d\phi$ where $P(\phi)$ is the experimental phase probability distribution.

[e] $R = \Sigma(|F_{obs}| - k|F_{calc}|) / \Sigma|F_{obs}|$. R_{free} value is the *R* value obtained for a test set of reflections, consisting of a randomly selected 10% subset of the diffraction data, not used during refinement (Brunger, 1992).

equivalent to those seen in structures of other G proteins bound to GppNHp and GDP (Dumas *et al*., 1999; Esters *et al*., 2000; Milburn *et al*., 1990; Pai *et al*., 1990; Tong *et al*., 1991).

Four additional Co^{2+} were included in the structure of Sec4-GDP; these were also identified using an anomalous difference map. Each is coordinated by side-chains from two Sec4 molecules, namely aspartate 43 and aspartate 166 from one molecule and histidine 121 from a neighboring molecule; the remaining ligands are ordered water molecules. This cobalt-mediated intermolecular bridging may explain the requirement for $CoCl_2$ for obtaining high-quality single crystals.

Sec4-GDP switch I region

Large, localized structural changes take place upon nucleotide hydrolysis (Figure 2(a) and (b)). Loss of the γ-phosphate eliminates two hydrogen bonds, between a phosphate oxygen atom and the side-chain hydroxyl group of threonine 51, and between a second phosphate oxygen group and the main-chain amide hydrogen atom of threonine

Table 2. Summary of crystallographic data for Sec4-GDP

A. *Data collection statistics*

	Inflection(λ1) 1	Peak (λ2) 1	High (λ3) 1	Inflection (λ1) 2	Peak (λ2) 2	High (λ3) 2
Wavelength (Å)	0.9797	0.9794	0.9796	0.9796	0.9794	0.9782
Resolution (Å)[a]	28.5-1.9(2.0-1.9)	28.5-1.9(2.0-1.9)	28.5-1.9(2.0-1.9)	28.5-1.9(2.0-1.9)	28.5-1.9(2.0-1.9)	28.5-1.9(2.0-1.9)
#observations	19,4983	19,5300	19,4067	23,8342	23,8422	23,8079
Unique	79,469	79,653	79,939	81,411	81,455	81,304
% complete	80.6(49.8)	80.8(50.8)	80.7(46.9)	82.1(41.4)	81.9(39.0)	82.1(42.5)
R_{sym}[b]	0.056(0.203)	0.056(0.212)	0.057(0.216)	0.064(0.289)	0.066(0.292)	0.067(0.290)
I/σ	12.6(4.2)	12.6(4.0)	12.5(4.0)	13.0(3.4)	12.0(3.5)	13.1(3.5)
a,*b*,*c*,α,β,γ	56.167,56.565,59.368,95.263,101.555,116.395			56.100,56.473,59.496,95.203,101.669,116.207		
Source/detector	ALS 5.0.2/Quantum-4			ALS 5.0.2/Quantum-4		

	Low (λ2) 3	Peak (λ1) 3
Wavelength (Å)	1.1000	0.9795
Resolution (Å)[a]	28.9-1.8(1.9-1.8)	28.9-1.9(2.0-1.9)
#observations	408214	376227
Unique	104861	95373
% complete	89.6(60.8)	95.8(95.9)
R_{sym}[b]	0.058(0.258)	0.066(0.351)
I/σ	20.0(5.2)	18.6(4.1)
a,*b*,*c*,α,β,γ	56.007,56.379,59.374,95.253,101.679,116.201	
Source/detector	ALS 5.0.2/Quantum-4	

B. *Anomalous phasing statistics*

MAD phasing power[c]

	λ_1-λ_1^-	λ_1-λ_2^+	λ_1-λ_2^-	λ_1-λ_3^+	λ_1-λ_3^-
Crystal 1, 28.5-1.9 Å (2.0-1.9 Å)	1.60 (0.73)	0.45 (0.22)	1.81 (0.81)	0.65 (0.27)	1.77 (0.80)
Crystal 2, 28.5-1.9 Å (2.0-1.9 Å)	1.55 (0.73)	0.55 (0.26)	1.78 (0.80)	0.80 (0.38)	1.70 (0.78)

SAD phasing power

	λ_1-λ_1^-
Crystal 3, 28.9-1.9 Å (2.0-1.9 Å)	0.73 (0.16)

Figures of merit[d]	28.9-1.9 Å (2.0-1.9 Å)
Crystal 1 MAD	0.48 (0.28)
Crystal 2 MAD	0.49 (0.28)
Crystal 3 SAD	0.16 (0.04)
Combined figure of merit	0.53 (0.24)

C. *Model statistics*

Resolution	28.9-1.8 Å (1.9-1.8 Å)	Luzatti coordinate error cross-validated (Å)	0.31 Å	# protein residues	640
R_{free}[e]	0.2964(0.3585)			# Co^{2+} ions	8
$R_{working}$	0.2761(0.3486)	Luzatti coordinate error Å	0.34	# GDP molecules	4
rms deviation, bonds (Å)	0.0064	σ_A coordinate error Å cross-validated	0.23	# water molecules	328
rms deviation, angles (deg.)	1.1325				
rms deviation, dihedrals (deg.)	22.5620	σ_A coordinate error (Å)	0.24		
rms deviation, impropers (deg.)	0.7090	average *B*-factor (Å^2)	32.2690		
most-favored phi-psi (%)	91.5	range of *B*-factors	10.6958-57.5458		

[a] Values in parentheses are for the high-resolution bin.

[b] $R_{sym} = \Sigma_h \Sigma_i |I_i(h) - \langle I(h)\rangle| / \Sigma_h \Sigma_i I_i(h)$ where $I_i(h)$ is the *i*th measurement and $\langle I(h)\rangle$ is the mean of all measurements of $I(h)$ for Miller indices *h*.

[c] MAD phasing power is defined as $[\langle |F_D - F_N|^2\rangle / \int_\phi P(\phi)(||F_N|e^{i\phi} + \Delta F_h| - |F_D|)^2 d\phi]^{1/2}$ where $P(\phi)$ is the experimental phase probability distribution. F_N corresponds to the structure factors at the reference wavelength, F_D corresponds to the structure factors at wavelength λ_i (indicated by a superscript +) or its Friedel mate (indicated by a superscript −), and ΔF_h is the difference in heavy atom structure factors between the two wavelengths. SAD phasing power is the same except the reference wavelength is λ_i.

[d] Figure of merit $= \int_\phi P(\phi) e^{i\phi} d\phi$ where $P(\phi)$ is the experimental phase probability distribution.

[e] $R = \Sigma(|F_{obs}| - k|F_{calc}|)/\Sigma|F_{obs}|$. R_{free} value is the *R* value obtained for a test set of reflections, consisting of a randomly selected 10% subset of the diffraction data, not used during refinement (Brunger, 1992).

52. As a result, residues 48 through 56 are displaced and disordered in Sec4-GDP. In molecule C this portion of the protein has weak, disconnected electron density and is greatly displaced relative to the structure of Sec4-GppNHp: the peptide bonds of residues 48 and 56 are flipped and the α-carbon of threonine 52 is moved by roughly 9 Å. In molecules A, B, and D, electron density in this region was too weak to be traced. We will refer to residues 48 through 56 of Sec4 as the switch I region, by analogy with Ras (Milburn *et al.*, 1990). This portion of Sec4 corresponds to residues 31 through 38 of Ras, as glycine 54 of Sec4 is a Rab family-specific insertion relative to Ras.

The switch I regions of Sec4-GDP and Ras-GDP do not overlap when the other residues in the two molecules are superimposed (Figure 3). The displacement of the switch I region of Sec4 following

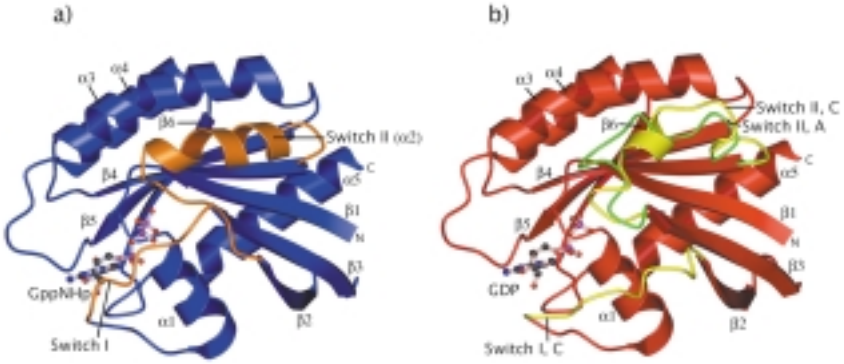

Figure 2. Structures of Sec4-GppNHp and Sec4-GDP. (a) Ribbon representation of Sec4-GppNHp, with secondary structure elements labeled. Regions of the protein structurally invariant with respect to Sec4-GDP are colored blue, and the switch I and II regions are colored orange. (b) Ribbon representation of Sec4 bound to GDP, with secondary structure elements labeled. Regions of the protein structurally similar among the four molecules in the unit cell, and invariant with respect to GppNHp-bound Sec4, are colored red. The switch II region of molecule A is colored green, and the switch I and II regions of molecule C are colored yellow. The switch I regions of molecules A, B, and D are disordered and were not included in the final model. The switch II regions of molecules B and D resemble the switch II regions of molecules A and C, respectively. (Figures 2, 3, 4(a) and (c) were prepared using the programs Molscript (Kraulis, 1991), GL_Render, and POV-RaY (POV-Ray Team, 1998).)

GTP hydrolysis is far greater than that of Ras, in which the α-carbon of threonine 35 (equivalent to threonine 52 in Sec4) is moved by only about 3.4 Å following GTP hydrolysis. In Ras-GDP the backbone carbonyl groups of residues 32, 33, and 34 in the switch I region accept hydrogen bonds from the water ligands of the Mg^{2+} (Milburn *et al.*, 1990; Tong *et al.*, 1991). Similar interactions are seen in the crystal structure of Rap2A-GDP (Cherfils *et al.*, 1997). These hydrogen bonds are absent in Sec4.

Sec4-GDP switch II region

Loss of the γ-phosphate group also leads to a rearrangement of residues 76-93 in Sec4 (Figure 2(a) and (b)), which we will refer to as the switch II region. The interaction between the switch I and switch II regions is disrupted when the switch I region becomes disordered following nucleotide hydrolysis. Loss of contacts between the switch I and switch II regions is the primary cause of the movement of the switch II region, as few contacts

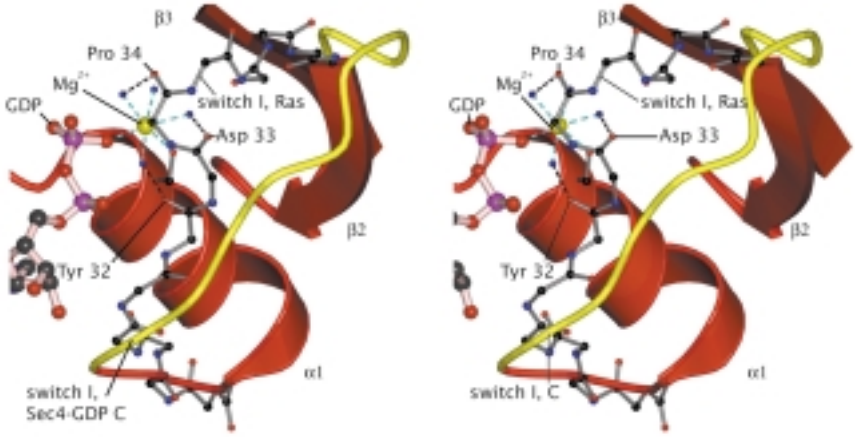

Figure 3. Stereoview comparing the switch I regions of Sec4-GDP and Ras-GDP, showing contacts between the peptide backbone of Ras (accession code 1Q21; Tong *et al.*, 1991) and water molecules involved in metal co-ordination. Similar contacts were seen in a second structure of Ras-GDP, accession code 4Q21 (Milburn *et al.*, 1990), and in the structure of Rap2A-GDP, accession code 1KAO (Cherfils *et al.*, 1997). Sec4-GDP is shown in red as a ribbon representation, with secondary structure elements labeled. The switch I region of molecule C is shown in yellow. The peptide backbone from Ras, including the switch I region and residues preceding it, is shown as a ball-and-stick representation superimposed on the structure of Sec4 (146 alpha carbon atoms superimposed with a rmsd of 1.1 Å). The nucleotide, metal ion, and water molecules from the Ras-GDP structure are shown. The nucleotide is drawn as a ball-and-stick representation. The metal ion is drawn as a yellow sphere, and the water molecules are drawn as blue spheres. Hydrogen bonds are shown as black broken lines, and the co-ordination of the metal ion is shown as cyan broken lines.

are made between residues in the switch II region of Sec4 and the γ-phosphate of the GppNHp. The only direct interaction between the switch II region and the γ-phosphate is a hydrogen bond between a phosphate oxygen atom and the backbone amide hydrogen atom of glycine 78. Loss of these interactions leads to movement of residues 76-81, already in a random coil, and partial unwinding of the irregular helix formed between residues 82 and 89. Residues 90-93 are also slightly displaced.

The switch II region of Sec4-GDP adopts two dramatically different conformations in the four molecules in the asymmetric unit (Figure 4(a)). The switch II regions of molecules A and B represent one conformation and the switch II regions of molecules C and D represent another. This portion of GDP-bound G proteins, especially small G proteins such as Ras, is often seen to be poorly ordered (Milburn *et al.*, 1990; Tong *et al.*, 1991). In our structure, this is the case for the first seven residues of the switch II region (residues 76 - 83) of molecule C. The next ten residues of molecule C (residues 84-93), however, exhibit well-connected and ordered electron density. By contrast, the first ten residues of the switch II region (residues 76-85) of molecule A are well ordered (Figure 4(b)), followed by eight residues (86-93) of less well-ordered electron density.

Conserved residues 76, 80, and 81 in the switch II region of molecule A face inwards towards the phosphates of the nucleotide. There they form a hydrogen-bonding network with side-chains from residues involved in nucleotide binding, and with water molecules that coordinate the metal ion (Figure 4(c)). The switch II region of molecule B appears to adopt a similar conformation and form similar interactions as molecule A, but the corresponding electron density is less ordered. The switch II region of molecule A will therefore form the basis for the description below:

The side-chain hydroxyl group of threonine 76 forms a hydrogen bond with a water molecule coordinating the cobalt ion, and with a side-chain oxygen atom from glutamate 80 (Figure 4(c)). Glutamate 80 also forms a hydrogen bond with the side-chain amino group of lysine 33, which in turn contacts the β-phosphate of the nucleotide. Arginine 81 makes a hydrogen bond with the side-chain from serine 29, which forms a long (3.6 Å) hydrogen bond with an oxygen atom from the β-phosphate. Arginine 81 also makes a long (3.7 Å) hydrogen bond with one of the water molecules coordinating the cobalt ion. A crystal packing contact is made by phenylalanine 82: the phenyl ring of the side-chain packs against the side-chain of proline 157 from a neighboring molecule. The contacts made by residues 76 and 80 closely resemble contacts made by residues threonine 66 and glutamate 70 from the switch II region of Ran-GDP. In Ran-GDP, however, the side-chain equivalent to arginine 81 of Sec4 (lysine 71) makes no contacts with water molecules coordinating the metal ion (Scheffzek *et al.*, 1995). The similarity between the structures of the switch II regions of Ran-GDP (Scheffzek *et al.*, 1995) and molecules A and B in our structure of Sec4-GDP suggests that the conformation of the switch II region that we observe is not an artifact of crystal packing.

In molecule C, the same residues adopt a conformation more reminiscent of the switch II regions of other GDP-bound G proteins including Ras (Milburn *et al.*, 1990; Tong *et al.*, 1991), Rap2A (Cherfils *et al.*, 1997), RhoA (Wei *et al.*, 1997), the alpha subunit of transducin (Lambright *et al.*, 1994), and Cdc42 bound to GDI and GDP (Hoffman *et al.*, 2000). Electron density in this region is disconnected, indicative of a disordered structure. Residues 76, 80, and 81 are flipped away from the nucleotide (Figure 4(a) and (c)) and face outwards. The side-chain of glutamate 80 forms a salt bridge with the side-chain of lysine 178 from molecule D, and the side-chain of arginine 81 donates a hydrogen bond to the backbone carbonyl group of phenylalanine 158 from molecule D. The phenyl ring of phenylalanine 82 also packs against the side-chain of proline 157 from a neighboring molecule. The side-chain hydroxyl group of threonine 76 forms a hydrogen bond with the side-chain hydroxyl group of tyrosine 89, possibly causing the ordering of the last ten residues of the switch II region of molecule C.

Discussion

The conservation of structural features of Sec4-GppNHp, Rab3A-GppNHp, and Ypt51-GppNHp (Dumas *et al.*, 1999; Esters *et al.*, 2000; Ostermeier & Brunger, 1999) suggest interactions specific for the Rab family of G proteins. The hydrogen bond between the side-chain of serine 29 and an oxygen atom from the γ-phosphate, seen in the Sec4, Rab3A, and Ypt51 structures, is probably the most significant interaction in terms of its effect on the low intrinsic GTP hydrolysis rates of Sec4 and Rab3A relative to the already low GTP hydrolysis rate of Ras. When this residue is mutated to glycine in Rab3A, the hydrolysis rate is increased threefold (Brondyk *et al.*, 1993). Conversely, when the equivalent glycine in Ras (glycine 12) is mutated to serine, intrinsic GTP hydrolysis is substantially decreased and cannot be activated by a GAP (Boguski & McCormick, 1993; McCormick, 1989; Trahey & McCormick, 1987). Additionally, the structure of the switch II region of active Rab proteins, which differs from that of active Ras, appears to be conserved (Dumas *et al.*, 1999; Esters *et al.*, 2000; Ostermeier & Brunger, 1999; Pai *et al.*, 1990).

The crystal structure of GTP-bound Rab3A in complex with the Rab3A-binding domain of Rabphilin-3A may serve as a model for the recognition of active Rab proteins by their effectors. In this structure, two non-contiguous areas of Rab3A are contacted by Rabphilin-3A: portions of the switch I and II regions, and a region including loops α2-β4

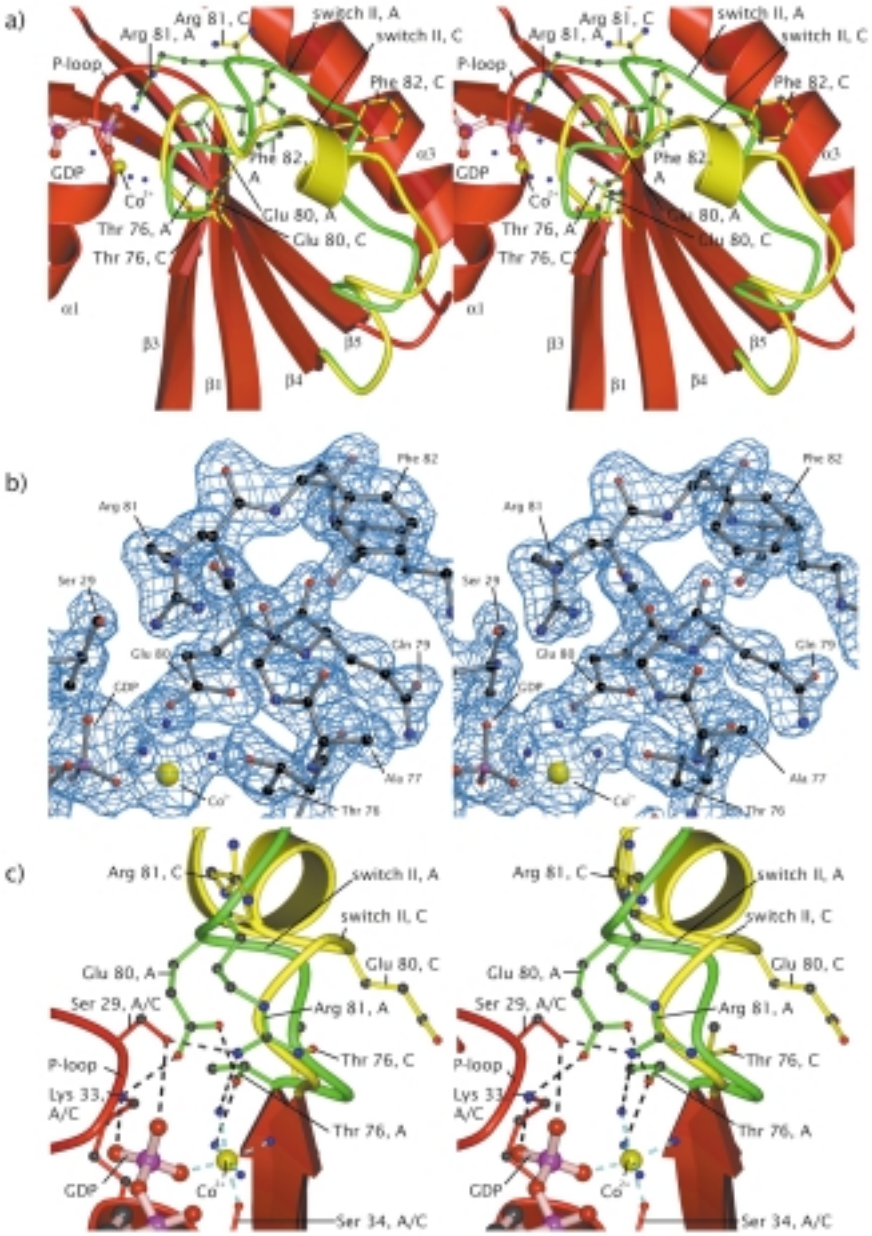

Figure 4. Structural differences between molecules A and C of Sec4-GDP. (a) Stereoview highlighting structural differences between the switch II regions of Sec4-GDP molecules A and C. The backbone trace of residues identical in both molecules is colored red. The backbone trace and ball-and-stick representations of selected side-chains in the switch II region of molecule A are colored green, while the backbone trace and ball-and-stick representations of selected side-chains in the switch II region of molecule C are colored yellow. Residues threonine 76, glutamate 80, and arginine 81 of molecule A point towards the phosphate groups of the nucleotide, while the same residues in molecule C point away from the nucleotide. The phenyl ring of phenylalanine 82 in all four molecules makes a crystal contact with the aliphatic carbon atoms of proline 157 in a neighboring molecule. (b) Stereoview of electron density from a phase-combined composite annealed omit map, contoured at 1.5 σ, near residues from the switch II region of Sec4-GDP molecule A. The nucleotide and protein residues from the final refined model are shown in a ball-and-stick representation. Water molecules are shown as blue spheres, and the bound metal ion is drawn as a yellow sphere. (c) Stereoview of the region near the phosphates of GDP bound by Sec4, showing the conserved residues from the switch II region that make contact with the residues and water molecules involved in binding the nucleotide and metal ion. The peptide backbone of Sec4 is shown as a continuous trace, and the side-chains of selected residues are represented as balls and sticks. The switch II region of molecule A is colored yellow, and the switch II region of molecule C is colored green. The cobalt ion is shown as a yellow sphere, and water molecules are shown as blue spheres. Hydrogen bonds are shown as black broken lines, and the coordination of the cobalt ion is shown as cyan broken lines.

and α3-β5, termed the Rab complementarity-determining region (Ostermeier & Brunger, 1999). Our structures of GppNHp- and GDP-bound Sec4 demonstrate that the conformational changes caused by GTP hydrolysis are confined to the switch I and switch II regions of Sec4. The remainder of the protein, including loops α2-β4 and α3-β5, is essentially unaffected by hydrolysis. This suggests that differing affinities of Rab effectors for GTP-bound and GDP-bound Rab proteins are due primarily to changes in the structures of the switch I and switch II regions following GTP hydrolysis. The Rab complementarity-determining region would then, as predicted, be expected to be involved in specific Rab-effector interactions, rather than in displaying the nucleotide-binding state of the Rab protein (Ostermeier & Brunger, 1999). It should be mentioned that a chimeric protein consisting of Sec4 with its α3-β5 loop replaced with the α3-β5 loop of Ypt1, a Rab protein involved in ER-Golgi transport in *S. cerevisiae*, is able to function as the sole copy of both Sec4 and Ypt1 in *S. cerevisiae* (Brennwald & Novick, 1993; Dunn *et al*., 1993). By indicating that the α3-β5 loop may be more important for effector recognition by Ypt1 than by Sec4, this result suggests that not all Rab-effector interactions take place in the same manner.

In Sec4-GDP, both the switch I and switch II regions are characterized by structural variability. The switch I region is highly disordered and displaced relative to the switch I region of Ras-GDP, leading to loss of contacts between residues in the switch I region and water molecules coordinating the metal ion (Milburn *et al*., 1990; Tong *et al*., 1991). Additionally, the switch II region of Sec4-GDP appears to be able to adopt two conformations. In the first, as seen in molecules A and B, residues threonine 76, glutamate 80, and arginine 81 from the switch II region make well-ordered contacts with other residues and water molecules important for metal and nucleotide binding (Figure 4(c)). In the second, as seen in molecules C and D, these residues are flipped away and make no contacts with groups involved in metal or nucleotide binding (Figure 4(c)).

We propose that the displacement and disorder in the switch I region and conformational variability in the switch II region of Sec4-GDP together lead to weakened metal binding by Sec4-GDP. Evidence for a link between the switch I region and metal binding by small G proteins is provided by a crystal structure of RhoA bound to GDP but without Mg^{2+}, in which the switch I region is displaced even more than in Sec4-GDP (Shimizu *et al*., 2000). Additionally, GDP binding by the closely related small G protein Cdc42 is promoted by RhoGDI, which stabilizes an interaction between the backbone carbonyl oxygen atom of a residue in the switch I region (threonine 35) and the Mg^{2+} (Hoffman *et al*., 2000).

Weak metal binding by Sec4-GDP may cause one property of Sec4 that differs from most other G proteins: a high off-rate (0.21 min^{-1} at 30 °C) for GDP, even at millimolar magnesium ion concentrations (Kabcenell *et al*., 1990). This is roughly an order of magnitude greater than the off-rate for GDP bound to Ras (0.025 min^{-1} at 37 °C) (Neal *et al*., 1988) and Rab3A (0.013 min^{-1} at 30 °C) (Burstein & Macara, 1992). A lowered affinity for Mg^{2+} could lead to a rapid off-rate for GDP, as the off-rate for nucleotides bound to G proteins is often much greater at very low free Mg^{2+} concentrations (Burstein & Macara, 1992; Hall & Self, 1986). Additionally, crystal structures of nucleotide-free G proteins (Ras, Arf1, and elongation factor-Tu) in complex with their guanine nucleotide exchange factors do not contain bound Mg^{2+} (Boriack-Sjodin *et al*., 1998; Goldberg, 1998; Kawashima *et al*., 1996; Wang *et al*., 1997).

It must be mentioned that in complexes of the small G proteins Ran and ADP ribosylation factor 1 (Arf1) with GDP, the switch I region does not interact with the nucleotide, the metal ion, or the ligands of the metal ion (Amor *et al*., 1994; Scheffzek *et al*., 1995). Despite this, the off-rate of GDP bound to these proteins is low relative to Sec4: 6×10^{-4} min^{-1} at 37 °C for Ran (Klebe *et al*., 1993) and 0.04 min^{-1} at 37 °C for [Δ17]Arf1, a variant of Arf1 with the first 17 residues removed (Menetrey *et al*., 2000; Paris *et al*., 1997). Other interactions may compensate for the lack of contacts with the switch I region. In Ran, residues threonine 66 and glutamate 70 from the switch II region make contacts with two water molecules coordinating the Mg^{2+} (Scheffzek *et al*., 1995). These contacts are equivalent to those made by residues 76 and 80 of Sec4. The switch II region of Ran-GDP, however, does not exhibit the conformational variability seen in Sec4-GDP (Scheffzek *et al*., 1995); this is the likely reason for the difference between the GDP off-rates of Sec4 and Ran (Kabcenell *et al*., 1990; Klebe *et al*., 1993).

In [Δ17]Arf1, glutamate 54 forms a seventh ligand for the Mg^{2+} (Amor *et al*., 1994); when this interaction is disrupted the off-rate of GDP bound to [Δ17]Arf1 increases threefold (Menetrey *et al*., 2000). Further evidence for the importance of this glutamate-metal contact for metal and nucleotide binding by Arf proteins is provided by the crystal structure of the complex between GDP and [Δ13]Arf6, a variant of Arf6 with its first 13 residues removed. In that structure, no interaction between the equivalent glutamate (glutamate 50) and the Mg^{2+} is observed (Menetrey *et al*., 2000). Accordingly, the off-rate of GDP bound to [Δ13]Arf6 is more than four times higher that that of GDP bound to [Δ17]Arf1 (Menetrey *et al*., 2000).

The possibility that the conformation of the switch II region of Sec4-GDP is determined by crystal packing contacts, particularly the interaction between the side-chains of phenylalanine 82 and proline 157, can not be excluded. Though the side-chains of residues 80, 81, and 82 in molecules C and D make contacts with residues from neighboring Sec4 molecules, the disordered structure in

residues 76-83 of molecules C and D suggests that these crystal packing contacts have little effect on the structure of the protein. In molecule A, residues 76, 80, and 81 make no contacts with neighboring molecules in the crystal. Furthermore, the structure in this region of molecule A is highly ordered (Figure 4(b)). Finally, the fact that a very similar conformation of the switch II region is seen in several structures of wild-type and mutant Ran proteins, both alone and in complex with nuclear transport factor 2, strongly suggests that the conformation of the switch II region in molecule A is not an artifact of crystal packing (Kent *et al*., 1999; Scheffzek *et al*., 1995; Stewart *et al*., 1998).

Stabilization of the potentially high-affinity interaction with metal ions and GDP seen in molecules A and B of the Sec4-GDP structure may be the mechanism by which GDI proteins reduce the off-rate of GDP bound to Sec4 and other Rab proteins. The residues in Cdc42 equivalent to residues 76, 80, and 81 of Sec4 are not in this conformation when Cdc42 is bound to GDP and RhoGDI (Hoffman *et al*., 2000). However, in the structure of Cdc42-GDP-RhoGDI, RhoGDI makes extensive contacts with residues from the switch II region (Hoffman *et al*., 2000). If the GDI that acts on Sec4 (Garrett *et al*., 1994) makes similar contacts with the switch II region, it may stabilize the interactions between residues 76, 80, and 81 and groups involved in metal and nucleotide binding. Additionally, RhoGDI interacts with the switch I region of Cdc42-GDP, stabilizing the interaction between the backbone carbonyl oxygen atom of threonine 35 and the Mg^{2+} (Hoffman *et al*., 2000). In a similar fashion, the GDI acting on Sec4 (Garrett *et al*., 1994) may stabilize the disordered switch I region of Sec4-GDP and allow it to participate in metal and/or nucleotide binding.

In summary, we have proposed that in Sec4-GDP a combination of displacement of the switch I region and structural variability in the switch II region causes weak Mg^{2+} binding by Sec4-GDP and leads to the high off-rate of GDP bound to Sec4. Additionally, we suggest that the mechanism of GDI action on Sec4-GDP involves stabilization of contacts between residues in the switch II region and groups important for nucleotide binding. GDI may also stabilize the switch I region of Sec4-GDP and allow it to participate in GDP binding. Mutational analysis and structural characterization of Sec4 and other Rab family members, as well as their regulatory proteins, will add further insight into the mechanisms by which nucleotide binding is regulated.

Materials and Methods

Protein preparation

Residues 19-187 of Sec4 were expressed as a glutathione-*S*-transferase (GST) fusion in *Escherichia coli* using the pGEX system (Pharmacia). *E. coli* cells of strain BL21 were transformed with the expression plasmid and grown to mid-log phase in terrific broth, then induced with 0.12 mM isopropyl-β-D-thiogalactopyranoside for three hours. Cells were harvested and resuspended into a buffer containing 20 mM Tris-HCl (pH 8.0), 5 mM $MgCl_2$, 100 mM NaCl, 1 mM DTT, 1 mM PMSF, and 0.01% (v/v) thesit, then lysed by sonication. Selenomethionine-substituted protein was also prepared in *E. coli* by inhibiting methionine biosynthesis in the presence of selenomethionine (Yu *et al*., 1999). After binding to glutathione-sepharose beads (Pharmacia), the Sec4 moiety was cleaved from the GST with bovine α-thrombin (Haematopoetic Technologies), then purified by anion-exchange (MonoQ resin) and size-exclusion (Superdex 75 resin) chromatography. The complex of Sec4 and guanosine-5′-(β,γ)-imidotriphosphate (GppNHp) was prepared by incubating Sec4 with a twofold molar excess of GppNHp and ten units calf intestinal alkaline phosphatase (Sigma) per milligram Sec4 in 20 mM Tris-HCl (pH 8.0), 5 mM $MgCl_2$, 1 mM DTT, and 100 mM NaCl at room temperature for 12 hours, followed by anion-exchange and size-exclusion chromatography. The complex of Sec4-GDP was prepared by incubating Sec4 at 4 °C for two to three weeks, or at room temperature for 24 hours, followed by anion-exchange and size-exclusion chromatography.

Crystallization, data collection, structure determination, and refinement of Sec4-GppNHp

Crystals of native Sec4-GppNHp were grown by mixing 2-5 μl of 25 mg/ml Sec4-GppNHp in 20 mM Tris-HCl (pH 8.0), 5 mM $MgCl_2$, 1 mM DTT, and 100 mM NaCl with the same volume of 25% (v/v) PEG 4000, 25-30% (v/v) ethylene glycol, 0.2 M $MgCl_2$, and 100 mM sodium Hepes (pH 7.7) and incubating for 12-18 hours at 21 °C in a hanging drop over 500 μl of 25% PEG 4000, 25-30% (v/v) ethylene glycol, 0.2 M $MgCl_2$, and 100 mM sodium Hepes (pH 7.7) in a sealed chamber. Microseeds were added and the drops were incubated at 21 °C for 24 hours. Crystals were removed from the drop with a nylon loop (Hampton Research) and flash-frozen directly in liquid propane, then stored in liquid nitrogen. Selenomethionine-substituted Sec4-GppNHp was crystallized in the same manner except that no ethylene glycol was present in the crystallization buffer; the crystals were transferred stepwise into 25% (v/v) PEG 400 in 5% increments, then frozen. Crystals of Sec4-GppNHp were hexagonal rods, in space group $P6_5$, with unit cell parameters $a = b = 84.504$ Å, $c = 86.469$ Å, $\alpha = \beta = 90°$, $\gamma = 120°$.

Anomalous diffraction data at four wavelengths, low-energy (0.9998 Å), inflection point (0.9802 Å), peak (0.9800 Å), and high-energy (0.9537 Å), was collected at beamline 5.0.2 at the Advanced Light Source on a selenomethionine-substituted crystal using a Quantum-4 (Area Detector Systems Corporation) CCD detector. Oscillation data at each wavelength was collected in 15° wedges, using inverse beam geometry, with data at each wavelength collected individually. Data was processed using DENZO and SCALEPACK (Otwinowski & Minor, 1997). Data on a native crystal was collected at a wavelength of 1.2843 Å at beamline X4A at the National Synchrotron Light Source. Oscillation data was collected using an R-AXIS IV (Rigaku Corporation) image plate detector and processed as above. Diffraction from the selenomethionine-labeled crystal extended to a minimum

Bragg spacing of 2.7 Å, and diffraction from the native crystal extended to minimum Bragg spacing of 2.0 Å.

The locations of the selenium atoms in the unit cell were determined by anomalous difference Fourier analysis using phases derived from a molecular replacement solution using two molecules of Rab3A as a search model. Peaks corresponding to positions of the six selenomethionine residues in the unit cell were found. This and all other calculations following data processing, except as noted, were carried out using the Crystallography and NMR System (CNS) (Brunger *et al.*, 1998).

Probably due to radiation damage during data collection, dispersive differences between the four MAD data sets were weak, and four-wavelength MAD phases calculated using the refined positions and *B*-factors of the anomalous scatterers were not useful (Burling *et al.*, 1996; Phillips & Hodgson, 1980). We then calculated two-wavelength MAD phases using the inflection point and edge data sets, and SAD phases from the inflection point, peak, and high-energy data sets, and combined the four phase sets. Density modification, consisting of solvent flipping, NCS averaging, and phase extension into the 2.0 Å native amplitudes (Abrahams & Leslie, 1996) resulted in electron density that was barely interpretable.

Refinement was carried out using the best solution of the translation search as a starting model, and consisted of several rounds of torsion angle simulated annealing (Rice & Brunger, 1994) and grouped and individual *B*-factor refinement (Hendrickson, 1985) using a maximum likelihood target function and including experimental phases (Pannu & Read, 1996), followed by manual rebuilding in O (Jones *et al.*, 1991). When refinement was carried out using a maximum likelihood target function, but without experimental phases, the R_{free} was 0.2945 and the $R_{working}$ was 0.2631. Without experimental phases, both *R*-factors were slightly higher, and the difference between R_{free} and $R_{working}$ was slightly greater, than in the presence of experimental phases. This result provides justification for our use of experimental phases during refinement. Refinement was carried out until the free and working *R*-factors had converged and residual $F_o - F_c$ maps contained no strong features. Non-crystallographic symmetry (NCS) restraints were included with a weight of 150. This weight was optimized using R_{free}. Residues 19-20, 62-68, 82-86, 94-95, 140, and 184-186 from both molecules were not included in the calculation of the NCS energy term. To reduce model bias, phase-combined composite annealed omit electron density maps were calculated. The nucleotide and magnesium ions were clearly visible in the electron density maps and were included early in the refinement process. Water molecules were picked automatically using phase-combined $2F_o - F_c$ and $F_o - F_c$ maps. Stereochemistry and geometry were assessed using CNS and PROCHECK (Laskowski *et al.*, 1993).

Crystallization, data collection, structure determination, and refinement of Sec4-GDP

Crystals of selenomethionine-labeled Sec4-GDP were grown by the microbatch method. Sec4-GDP (2.5 µl) in 20 mM Tris-HCl (pH 8.0) and 5 mM $MgCl_2$ were mixed with 2.5 µl of 12% (v/v) PEG 4000, 70 mM $CoCl_2$, and 100 mM sodium cacodylate (pH 5.7), and incubated in a hanging drop for 16-20 hours at 10°C in a sealed chamber. Crystals were removed from the drop with a nylon loop and vigorously passed through perfluoropolyether vacuum-pump oil (FOMBLIN®, Aldrich Chemical Co.) several times until most of the aqueous mother liquor had been removed. The crystals were then flash frozen as described above. Crystals of Sec4-GDP were in space group *P*1, with unit cell parameters $a = 56.007$ Å, $b = 56.379$ Å, $c = 59.374$ Å, $\alpha = 95.253°$, $\beta = 101.679°$, $\gamma = 116.201°$.

While a molecular replacement solution was found using four molecules of Sec4-GppNHp as a search model, the resulting phases were insufficient to resolve the switch I and switch II regions. Therefore, a MAD experiment was carried out. Anomalous diffraction data was collected on two crystals of selenomethionine-labelled Sec4-GDP, at three wavelengths each: inflection point (0.9797/0.9796 Å), peak (0.9794/0.9794 Å), and high-energy (0.9778/0.9782 Å) at beamline 5.0.2 at the Advanced Light Source using a Quantum-4 CCD detector. Oscillation data at each wavelength was collected using inverse-beam geometry in 20° wedges, with data in each wedge collected at all three energies before moving to the next wedge. Data was collected, also using inverse-beam geometry in 20° wedges, on a third crystal, at the peak wavelength (0.9795 Å) and a low-energy wavelength (1.1 Å).

The sites of anomalous scatterers, namely selenium and cobalt, were found by anomalous difference Fourier analysis using phases derived from a molecular replacement solution using four molecules of Sec4-GppNHp as a search model. Positions and *B*-factors of the strongest 12 peaks in an anomalous difference map were refined and MAD phases calculated. Five additional sites were found using residual gradient maps (Bricogne, 1984). The positions and *B*-factors of all sites were refined, and MAD phases extending to 1.9 Å resolution were again calculated from each of the two MAD experiments. SAD phases to 1.9 Å resolution were calculated from the data collected at the peak wavelength on the third crystal. These three phase probability distributions were then combined. Density modification, consisting of solvent flipping, NCS averaging, and phase extension to 1.8 Å resolution, using amplitudes of the low-energy data from the third crystal, was carried out, resulting in interpretable electron density.

Refinement, using the solution of the translation search as a starting model, consisted of several rounds of torsion angle dynamics simulated annealing (Rice & Brunger, 1994) and grouped and individual *B*-factor refinement (Hendrickson, 1985) using a maximum-likelihood target function and including experimental phases (Pannu & Read, 1996), followed by manual rebuilding using O (Jones *et al.*, 1991). Experimental phases were necessary for successful refinement of the structure. Refinement was carried out until the free and working *R*-factors had converged and residual $F_o - F_c$ maps contained no strong features. NCS symmetry was included with a weight of 80; this weight was optimized using R_{free}. The switch I and II regions from all four molecules were not included in calculating the NCS energy term. The nucleotide and cobalt ions were clearly visible in phase-combined $2F_o - F_c$ maps and were included early in the refinement process. Water molecules were picked automatically from $2F_o - F_c$ and $F_o - F_c$ maps. Stereochemistry and geometry were assessed using CNS and PROCHECK (Laskowski *et al.*, 1993).

Protein Data Bank accession code

The coordinates have been deposited in the RCSB Protein Data Bank, with accession codes 1G16 (Sec4-GDP) and 1G17 (Sec4-GppNHp).

Acknowledgments

We thank T. Earnest, L.-W. Hung, J. Ernst, R.Yu, and L. Rice for assistance in data collection at beamline 5.0.2 at the Advanced Light Source (ALS), C. Ogata and M. Wilson for assistance in data collection at beamline X4A at the National Synchrotron Light Source (NSLS), P. Novick, R.B. Sutton, P. D. Adams, and R. Grosse-Kunstleve for discussion and expert advice, and L. Rice, J. Hyman, M. Kercher, and K. Slep for critical reading of this manuscript.

References

Abrahams, J. P. & Leslie, A. G. W. (1996). Methods used in the structure determination of bovine mitochondrial F_1 ATPase. *Acta Crystallog. ser D,* **52**, 30-42.

Amor, J. C., Harrison, D. H., Kahn, R. A. & Ringe, D. (1994). Structure of the human ADP-ribosylation factor-1 complexed with GDP. *Nature,* **372**, 704-708.

Boguski, M. S. & McCormick, F. (1993). Proteins regulating Ras and its relatives. *Nature,* **366**, 643-654.

Boriack-Sjodin, P. A., Margarit, S. M., Bar-Sagi, D. & Kuriyan, J. (1998). The structural basis of the activation of Ras by Sos. *Nature,* **394**, 337-343.

Bourne, H. R., Sanders, D. A. & McCormick, F. (1990). The GTPase superfamily: a conserved switch for diverse cell functions. *Nature,* **348**, 125-132.

Bourne, H. R., Sanders, D. A. & McCormick, F. (1991). The GTPase superfamily: conserved structure and molecular mechanism. *Nature,* **349**, 117-127.

Brennwald, P. & Novick, P. (1993). Interactions of 3 domains distinguishing the Ras-related GTP-binding proteins Ypt1 and Sec4. *Nature,* **362**, 560-563.

Bricogne, G. (1984). Maximum entropy and the foundations of direct methods. *Acta Crystallog. ser A,* **40**, 410-445.

Brondyk, W. H., McKiernan, C. J., Burstein, E. S. & Macara, I. G. (1993). Mutants of Rab3A analogous to oncogenic Ras mutants: sensitivity to Rab3A-GTPase activating protein and Rab3A-guanine nucleotide releasing factor. *J. Biol. Chem.* **268**, 9410-9415.

Brunger, A. T. (1992). Free *R* value: a novel statistical quantity for assessing the accuracy of crystal structures. *Nature,* **355**, 472-475.

Brunger, A. T., Adams, P. D., Clore, G. M., DeLano, W. L., Gros, P., Grosse-Kunstleve, R. W., Jiang, J. S., Kuszewski, J., Nilges, M., Pannu, N. S., Read, R. J., Rice, L. M., Simonson, T. & Warren, G. L. (1998). Crystallography and NMR system: a new software suite for macromolecular structure determination. *Acta Crystallog. ser D,* **54**, 905-921.

Burling, F. T., Weis, W. I., Flaherty, K. M. & Brunger, A. T. (1996). Direct observation of protein solvation and discrete disorder with experimental crystallographic phases. *Science,* **271**, 72-77.

Burstein, E. S. & Macara, I. G. (1992). Interactions of the ras-like protein-$p25^{rab3A}$ with Mg^{2+} and guanine nucleotides. *Biochem. J.* **282**, 387-392.

Cherfils, J., Menetrey, J., Le Bras, G., Janoueix-Lerosey, I., de Gunzburg, J., Garel, J. R. & Auzat, I. (1997). Crystal structures of the small G protein Rap2A in complex with its substrate GTP, with GDP and with GTPγ S. *EMBO J.* **16**, 5582-5591.

Du, L. L., Collins, R. N. & Novick, P. J. (1998). Identification of a Sec4p GTPase activating protein (GAP) as a novel member of a Rab GAP family. *J. Biol. Chem.* **273**, 3253-3256.

Dumas, J. J., Zhu, Z. Y., Connolly, J. L. & Lambright, D. G. (1999). Structural basis of activation and GTP hydrolysis in Rab proteins. *Struct. Fold. Design,* **7**, 413-423.

Dunn, B., Stearns, T. & Botstein, D. (1993). Specificity domains distinguish the Ras-related GTPases Ypt1 and Sec4. *Nature,* **362**, 563-565.

Esnouf, R. M. (1997). An extensively modified version of Molscript that includes greatly enhanced coloring capabilities. *J. Mol. Graph. Model.* **15**, 132.

Esters, H., Alexandrov, K., Constantinescu, A. T., Goody, R. S. & Scheidig, A. J. (2000). High-resolution crystal structure of S. cerevisiae Ypt(ΔC15)-GppNHp, a small GTP-binding protein involved in regulation of endocytosis. *J. Mol. Biol.* **298**, 111-121.

Garrett, M. D., Zahner, J. E., Cheney, C. M. & Novick, P. J. (1994). *GDI1* encodes a GDP dissociation inhibitor that plays an essential role in the yeast secretory pathway. *EMBO J.* **13**, 1718-1728.

Geyer, M. & Wittinghofer, A. (1997). GEFs, GAPs, GDIs and effectors: taking a closer (3D) look at the regulation of Ras-related GTP binding proteins. *Curr. Opin. Struct. Biol.* **7**, 786-792.

Goldberg, J. (1998). Structural basis for activation of ARF GTPase: mechanisms of guanine nucleotide exchange and GTP-myristoyl switching. *Cell,* **95**, 237-248.

Guo, W., Roth, D., Walch-Solimena, C. & Novick, P. (1999). The exocyst is an effector for Sec4p, targeting secretory vesicles to sites of exocytosis. *EMBO J.* **18**, 1071-1080.

Hall, A. & Self, A. J. (1986). The effect of Mg^{2+} on the guanine nucleotide exchange rate of $p21^{N\text{-}ras}$. *J. Biol. Chem.* **261**, 963-965.

Hendrickson, W. A. (1985). Stereochemically restrained refinement of macromolecular structures. *Methods Enzymol.* **115**, 252-270.

Hoffman, G. R., Nassar, N. & Cerione, R. A. (2000). Structure of the Rho family GTP-binding protein Cdc42 in complex with the multifunctional regulator RhoGDI. *Cell,* **100**, 345-356.

Jones, T. A., Zou, J. Y., Cowan, S. W. & Kjeldgaard, M. (1991). Improved methods for building protein models in electron density maps and the location of errors in these models. *Acta Crystallog. ser A,* **47**, 110-119.

Kabcenell, A. K., Goud, B., Northup, J. K. & Novick, P. J. (1990). Binding and hydrolysis of guanine nucleotides by Sec4p, a yeast protein involved in the regulation of vesicular traffic. *J. Biol. Chem.* **265**, 9366-9372.

Kawashima, T., Berthet-Colominas, C., Wulff, M., Cusack, S. & Leberman, R. (1996). The structure of the *Escherichia coli* EF-TU·EF-Ts complex at 2.5 Å resolution. *Nature,* **379**, 511-518.

Kent, H. M., Moore, M. S., Quimby, B. B., Baker, A. M. E., McCoy, A. J., Murphy, G. A., Corbett, A. H. & Stewart, M. (1999). Engineered mutants in the switch II loop of Ran define the contribution made by key residues to the interaction with

nuclear transport factor 2 (NTF2)and the role of this interaction in nuclear protein import. *J. Mol. Biol.* **289**, 565-577.

Klebe, C., Nishimoto, T. & Wittinghofer, F. (1993). Functional expression in *Escherichia coli* of the mitotic regulator proteins $p24^{ran}$ and $p45^{rcc1}$ and fluorescence measurements of their interaction. *Biochemistry,* **32**, 11923-11928.

Kraulis, P. J. (1991). Molscript: a program to produce both detailed and schematic plots of protein structures. *J. Appl. Crystallog.* **24**, 946-950.

Lambright, D. G., Noel, J. P., Hamm, H. E. & Sigler, P. B. (1994). Structural determinants for activation of the α subunit of a heterotrimeric G protein. *Nature,* **369**, 621-628.

Laskowski, R. A., Macarthur, M. W., Moss, D. S. & Thornton, J. M. (1993). PROCHECK: a program to check the stereochemical quality of protein structures. *J. Appl. Crystallog.* **26**, 283-291.

Martinez, O. & Goud, B. (1998). Rab proteins. *Biochim. Biophys. Acta Mol. Cell Res.* **1404**, 101-112.

McCormick, F. (1989). *ras* GTPase activating protein: signal transmitter and signal terminator. *Cell,* **56**, 5-8.

Menetrey, J., Macia, E., Pasqualato, S., Franco, M. & Cherfils, J. (2000). Structure of Arf6-GDP suggests a basis for guanine nucleotide exchange factors specificity. *Nature Struct. Biol.* **7**, 466-469.

Metalloprotein Structure Design Group. (1998). MDB (Main Page) - Metalloprotein site aatabase & browser, TSRI. In *Metalloprotein site Database and Browser (MDB), Release 1.3* (http://metallo. scripps. edu/) .

Milburn, M. V., Tong, L., Devos, A. M., Brunger, A., Yamaizumi, Z., Nishimura, S. & Kim, S. H. (1990). Molecular switch for signal transduction: structural differences between active and inactive forms of protooncogenic *ras* proteins. *Science,* **247**, 939-945.

Neal, S. E., Eccleston, J. F., Hall, A. & Webb, M. R. (1988). Kinetic analysis of the hydrolysis of GTP by $p21^{N\text{-}ras}$: the basal GTPase mechanism. *J. Biol. Chem.* **263**, 19718-19722.

Newman, C. M. H. & Magee, A. I. (1993). Posttranslational processing of the Ras superfamily of small GTP-binding proteins. *Biochim. Biophys. Acta,* **1155**, 79-96.

Novick, P. & Brennwald, P. (1993). Friends and family: the role of the Rab GTPases in vesicular traffic. *Cell,* **75**, 597-601.

Novick, P., Brennwald, P., Walworth, N. C., Kabcenell, A. K., Garrett, M., Moya, M., Roberts, D., Muller, H., Govindan, B. & Bowser, R. (1993). The cycle of Sec4 function in vesicular transport. In *GTPase Superfamily*, vol. 176, pp. 218-228, John Wiley and Sons, Chichester, UK.

Ostermeier, C. & Brunger, A. T. (1999). Structural basis of Rab effector specificity: crystal structure of the small G protein Rab3A complexed with the effector domain of Rabphilin-3A. *Cell,* **96**, 363-374.

Otwinowski, Z. & Minor, W. (1997). Processing of X-ray diffraction data collected in oscillation mode. *Macromolecular Crystallography, Part A,* **276**, 307-326.

Pai, E. F., Krengel, U., Petsko, G. A., Goody, R. S., Kabsch, W. & Wittinghofer, A. (1990). Refined crystal structure of the triphosphate conformation of H-*ras* p21 at 1.35 Å resolution - implications for the mechanism of GTP hydrolysis. *EMBO J.* **9**, 2351-2359.

Pannu, N. S. & Read, R. J. (1996). Improved structure refinement through maximum likelihood. *Acta Crystallog. ser. A,* **52**, 659-668.

Paris, S., BeraudDufour, S., Robineau, S., Bigay, J., Antonny, B., Chabre, M. & Chardin, P. (1997). Role of protein-phospholipid interactions in the activation of ARF1 by the guanine nucleotide exchange factor Arno. *J. Biol. Chem.* **272**, 22221-22226.

Pfeffer, S. R. (1994). Rab GTPases - master regulators of membrane trafficking. *Curr. Opin. Cell Biol.* **6**, 522-526.

Phillips, J. C. & Hodgson, K. O. (1980). The use of anomalous scattering effects to phase diffraction patterns from macromolecules. *Acta Crystallog. ser. A,* **36**, 856-864.

POV-Ray, Team. (1998). POV-Ray: the persistence of vision raytracer. (http://www. povray. org/) Cyborg Software Systems, Indianapolis, IN.

Rice, L. M. & Brunger, A. T. (1994). Torsion angle dynamics: reduced variable conformational sampling enhances crystallographic structure refinement. *Proteins: Struct. Funct. Genet.* **19**, 277-290.

Salminen, A. & Novick, P. J. (1987). A *ras*-like protein is required for a post-Golgi event in yeast secretion. *Cell,* **49**, 527-538.

Scheffzek, K., Klebe, C., Fritzwolf, K., Kabsch, W. & Wittinghofer, A. (1995). Crystal structure of the nuclear Ras-related protein Ran in its GDP-bound form. *Nature,* **374**, 378-381.

Scheffzek, K., Ahmadian, M. R. & Wittinghofer, A. (1998). GTPase-activating proteins: helping hands to complement an active site. *Trends Biochem. Sci.* **23**, 257-262.

Shimizu, T., Ihara, K., Maesaki, R., Kuroda, S., Kaibuchi, K. & Hakoshima, T. (2000). An open conformation of switch I revealed by the crystal structure of a Mg^{2+}-free form of RhoA complexed with GDP. *J. Biol. Chem.* **275**, 18311-18317.

Sprang, S. R. (1997). G protein mechanisms: insights from structural analysis. *Annu. Rev. Biochem.* **66**, 639-678.

Stewart, M., Kent, H. M. & McCoy, A. J. (1998). Structural basis for molecular recognition between nuclear transport factor 2 (NTF2) and the GDP-bound form of the Ras-family GTPase Ran. *J. Mol. Biol.* **277**, 635-646.

Tong, L., Devos, A. M., Milburn, M. V. & Kim, S. H. (1991). Crystal structures at 2. 2 Å resolution of the catalytic domains of normal *ras* protein and an oncogenic mutant complexed with GDP. *J. Mol. Biol.* **217**, 503-516.

Trahey, M. & McCormick, F. (1987). A cytoplasmic protein stimulates normal N-*ras* p21 GTPase, but does not affect oncogenic mutants. *Science,* **238**, 542-545.

Walch-Solimena, C., Collins, R. N., Govindan, B. & Novick, P. (1996). Sec2p acts in conjunction with Sec4p to target secretory vesicles in yeast. *Mol. Biol. Cell,* **7**, 2562-.

Walch-Solimena, C., Collins, R. N. & Novick, P. J. (1997). Sec2p mediates nucleotide exchange on Sec4p and is involved in polarized delivery of post-Golgi vesicles. *J. Cell Biol.* **137**, 1495-1509.

Walworth, N. C., Goud, B., Kabcenell, A. K. & Novick, P. J. (1989). Mutational analysis of Sec4 suggests a cyclical mechanism for the regulation of vesicular traffic. *EMBO J.* **8**, 1685-1693.

Wang, Y., Jiang, Y. X., MeyeringVoss, M., Sprinzl, M. & Sigler, P. B. (1997). Crystal structure of the EF-

Tu·EF-Ts complex from *Thermus thermophilus*. *Nature Struct. Biol.* **4**, 650-656.

Wei, Y. Y., Zhang, Y., Derewenda, U., Liu, X. P., Minor, W., Nakamoto, R. K., Somlyo, A. V., Somlyo, A. P. & Derewenda, Z. S. (1997). Crystal structure of RhoA-GDP and its functional implications. *Nature Struct. Biol.* **4**, 699-703.

Yu, R. C., Jahn, R. & Brunger, A. T. (1999). NSF N-terminal domain crystal structure: models of NSF function. *Mol. Cell,* **4**, 97-107.

Edited by D. Rees

(Received 7 August 2000; received in revised form 12 October 2000; accepted 13 October 2000)